

# NATIONAL ADVISORY COMMITTEE FOR AERONAUTICS

NACA-TECHNICAL NOTE

No. 1354

COMPARISON OF SOUND EMISSION FROM TWO-BLADE, FOUR-BLADE,  
AND SEVEN-BLADE PROPELLERS

By Chester W. Hicks and Harvey H. Hubbard

Langley Memorial Aeronautical Laboratory  
Langley Field, Va.



Washington

July 1947

1000

NATIONAL ADVISORY COMMITTEE FOR AERONAUTICS

TECHNICAL NOTE NO. 1354

COMPARISON OF SOUND EMISSION FROM TWO-BLADE, FOUR-BLADE,  
AND SEVEN-BLADE PROPELLERS

By Chester W. Hicks and Harvey H. Hubbard

SUMMARY

Measurements of sound pressures for static conditions are presented for two-blade, four-blade, and seven-blade propellers in the tip Mach number range 0.3 to 0.9. The experimental results were found to check satisfactorily with those calculated by means of Gutin's formula for the whole Mach number range in the case of the two-blade propeller. Good agreement was obtained in the case of the seven-blade propeller for Mach numbers above 0.5, but large discrepancies were found to exist in the Mach number range below 0.5. Vortex noise is a large part of the total noise at low tip Mach numbers, especially for multiblade propellers, and therefore Gutin's formula is inaccurate for these conditions. Despite the discrepancies noted, an appreciable sound-pressure reduction may be realized by changing from a two-blade propeller to a seven-blade propeller for comparable operating conditions.

Tests completed of 2 two-blade propellers having different solidity indicate that solidity has very little if any effect on sound-pressure emission of two-blade propellers. At a fixed-pitch setting the sound-intensity levels expressed in decibels are approximately a linear function of tip speed for the test Mach number range for all propellers tested.

Gutin's formula for the calculation of sound pressures from an airplane propeller has been simplified for use in engineering work by conversion from metric to British Engineering units. A sample problem illustrating the use of Gutin's formula is included. Measured and calculated results for several propellers are compared.

For the same tip speed and power absorbed, a seven-blade propeller is only slightly less loud than a two-blade propeller at distances greater than 400 feet even though the difference in sound pressures is large. For the same tip speed and power absorbed, a small reduction in loudness may be realized by increasing the diameter and, hence, decreasing the frequency of the emitted sound. Two sample calculations illustrating the Fletcher-Munson method of loudness evaluation are included.

## INTRODUCTION

Much interest has been shown recently in the problem of noise reduction of light airplanes. Theodorsen and Regier (reference 1) concluded that propeller noise for commonly used tip speeds is the dominant part of all noise created by a propeller-driven airplane and have treated the problem according to the theory developed by Gutin in reference 2. Deming (reference 3) checked the Gutin theory for two-blade propellers. From these checks it was concluded that the theory was satisfactory, at least for two-blade propellers, although it tended to underestimate the energy in the higher harmonics. With the application of the theory to fan-type propellers further test work appeared desirable to extend the range of experimental checks against theory. Tests have therefore been made for a series of different propellers including two-blade, four-blade, and seven-blade configurations.

Noise from airplane propellers is known to be complex and its breakdown into individual parts is difficult. The two parts that are considered are (1) rotational noise and (2) vortex noise. Rotational noise is caused by rotation of the steady pressure field enveloping each blade, whereas vortex noise is caused by oscillatory disturbances in the flow around the propeller blade.

Although the Gutin theory predicts sound pressures due to rotational noise, it does not provide means for predicting vortex noise or evaluating the loudness of complex sounds. Measurements of the sound intensity by electrical instruments give a physical value of its magnitude, but the intensity evaluated by the ear is physiological and psychological and gives a loudness value. Two important factors that affect the loudness of propeller noise are the presence of vortex noise and the nonlinear response of the ear to the frequency spectrum. The purpose of the present analysis is therefore to investigate the loudness of propeller noises as heard by the ear as well as to check the Gutin theory for sound pressure emission.

## SYMBOLS

|       |   |
|-------|---|
| $P_1$ | root-mean-square sound pressure, dynes per square centimeter (bars) |
| $n$   | number of blades  |
| $q$   | harmonic of sound   |

|             |   |
|-------------|---|
| $\omega$    | speed of revolution, radians per second                                       |
| $c$         | velocity of sound, feet per second  |
| $s$         | distance from propeller, feet   |
| $T$         | thrust, pounds  |
| $Q$         | torque, pound-feet  |
| $\beta$     | angle from propeller axis of rotation (zero in front)                         |
| $R$         | propeller mean radius, feet   |
| $V$         | velocity of propeller section at radius $R$ , feet per second                 |
| $J_{qn}(x)$ | Bessel function of order $qn$ and argument<br>$x = qn \frac{V}{c} \sin \beta$ |
| $B_{qn}$    | $B_{qn} = qn J_{qn} \left( qn \frac{V}{c} \sin \beta \right)$                 |
| $M_t$       | tip Mach number of blade (rotation only)                                      |
| $M$         | Mach number of section at $R$   |
| $R_t$       | radius of propeller to tip  |
| $A$         | area of disk with radius $R_t$  |
| $P$         | power supplied to propeller, foot-pounds per second                           |
| $P_H$       | horsepower supplied to propeller  |
| $I$         | sound-pressure level, decibels  |
| $P_T$       | summation of harmonic sound pressure emissions                                |
| $b/D$       | blade-width ratio   |
| $h/b$       | blade-thickness ratio   |
| $\theta$    | blade angle, degrees  |
| $b$         | blade chord, feet   |

|            |   |
|------------|---|
| D          | propeller diameter, feet  |
| h          | blade-section maximum thickness, feet   |
| r          | radius to a blade element, feet   |
| k          | order of the harmonic   |
| $\psi_k$   | sound-pressure level of kth harmonic, decibels  |
| $b_k$      | masking factor  |
| $G_k$      | loudness function   |
| $L_n$      | loudness of a steady complex tone having n components   |
| $f_k$      | frequency of the kth component, cycles per second   |
| $f_m$      | frequency of the masking component, cycles per second   |
| $L_k$      | loudness level of the kth component when sounding alone   |
| $L_m$      | loudness level of the masking tone  |
| Z          | function depending on the sound-pressure level $\psi_k$ and the frequency $f_k$ of each component (given in table IV as a function of $X = \psi_k + 30 \log f_k - 95$ ) |
| U          | masking coefficient (given by the curve of fig. 12)   |
| Subscript: |   |
| l          | quantities expressed in metric units (dynes, centimeters, seconds)  |

### SOUND THEORY

Propeller sound can be considered to consist of vortex noise and rotational noise. The vortex noise is caused by oscillating disturbances in the flow around the propeller blade. Frequencies of vortex noise form a continuous spectrum from near zero frequency to frequencies of several thousand cycles per second, the upper limit depending on the rotational speed and size of the propeller blade (reference 4). These sounds do not register as pure tones but combine to produce a "tearing sound" to the observer.

Rotational noise is caused by the rotation of the steady pressure field enveloping each blade. A theory was developed by Gutin (reference 2) with reference to these steady aerodynamic forces on the blade. Gutin assumes that no forces act on the air until the blade reaches the air and that energy is imparted suddenly at each blade passage. Thus, the air receives energy from the blade in impulses having the shape of a square wave, which can be resolved into its Fourier coefficients. The frequencies of the sound produced are therefore integral multiples of the fundamental frequency of blade passage (rotational frequency multiplied by the number of blades).

The formula for the rotational sound pressure from an airplane propeller at low forward speeds as developed by Gutin (reference 2) is as follows:

$$p_1 = \frac{qn\omega}{2\sqrt{2} \pi c_1 s_1} \left( -T_1 \cos \beta + \frac{c_1 Q_1}{\omega R_1^2} \right) J_{qn} \sin \beta \frac{V_1}{c_1} \quad (1)$$

where pressure is given in dynes per square centimeter when all units are in the metric system. By substituting  $B_{qn}$  for  $qnJ_{qn}(x)$ , where  $x = qn \frac{V_1}{c_1} \sin \beta$ , equation (1) becomes

$$p_1 = \frac{\omega}{2\sqrt{2} \pi c_1 s_1} \left( -T \cos \beta + \frac{c_1 Q_1}{\omega R_1^2} \right) B_{qn}$$

Changing the right side of this equation to British Engineering units (feet, pounds) gives

$$p_1 = \frac{169.3\omega}{\pi c s} \left( -T \cos \beta + \frac{c Q}{\omega R^2} \right) B_{qn}$$

In reference 1 sound pressures were evaluated in terms of the propeller thrust and airplane speed. In the present analysis the formula for the sound pressure is expressed in terms of thrust and horsepower, a form more convenient for determining sound pressures from an airplane propeller operating at zero forward speed and in the take-off condition.

Multiplying the numerator and the denominator of the preceding equation by  $R_t^2$  gives

$$p_1 = \frac{169.3 \omega R_t^2}{c \pi R_t^2} \left( -T \cos \beta + \frac{cQ}{\omega R^2} \right) B_{qn}$$

or, in terms of tip Mach number  $M_t$  and disk area  $A$ ,

$$p_1 = 169.3 \frac{M_t R_t}{sA} \left( -T \cos \beta + \frac{cQ}{\omega R^2} \right) B_{qn}$$

Since  $Q = \frac{P}{\omega}$ ,

$$p_1 = 169.3 \frac{M_t R_t}{sA} \left( -T \cos \beta + \frac{cP}{\omega^2 R^2} \right) B_{qn}$$

Multiplying the power term by  $c/c$  gives

$$p_1 = 169.3 \frac{M_t R_t}{sA} \left( -T \cos \beta + \frac{c^2 P}{\omega^2 R^2 c} \right) B_{qn}$$

Hence,

$$p_1 = 169.3 \frac{M_t R_t}{sA} \left( -T \cos \beta + \frac{P}{M^2 c} \right) B_{qn} \quad (2)$$

Equation (2) is convenient for engineering use.

For the tests reported herein,  $\beta = 105^\circ$ . This particular angular position was chosen because it is near the axis of maximum sound pressures for the range of rotational noise frequencies measured. The value of  $c$  was taken as 1126 feet per second, a value corresponding approximately to test conditions. It is also assumed for all calculations that  $M = 0.8M_t$ , since this value gives better correlation with experimental results than other values used. Substituting these constants into equation (2) and changing  $P$  to horsepower gives

$$p_1 = 169.3 \frac{M_t R_t}{sA} \left( 0.26T + \frac{0.76P_H}{M_t^2} \right) qn J_{qn} (0.77 M_t qn) \quad (3)$$



Equation (3) was used in evaluating test results. The sound pressure for any propeller may be calculated if the thrust and the power absorbed can be determined. As calculated by equations (2) and (3),  $p_1$  is the sound pressure in free space. In general, ground reflection causes a doubling of the sound intensities at the ground level; hence, values obtained by equations (2) and (3) were doubled for comparison with experimental results.

From the information given in reference 5, the root-mean-square pressure of 1 dyne per square centimeter is shown in reference 1 to correspond to a sound level of 74 decibels and the sound level at a pressure  $p_1$  in dynes per square centimeter is

$$I = 74 + 20 \log_{10} p_1 \text{ decibels}$$

The total pressure of several harmonics may be obtained by extracting the square root of the sum of their squares (reference 1); thus

$$p_T = \sqrt{\sum_q p_1^2}$$

and the total sound-pressure level in decibels is

$$I = 74 + 20 \log_{10} \sqrt{\sum_q p_1^2} \quad (4)$$

If atmospheric attenuation is neglected, the sound pressure varies inversely as the distance (equation (1)). Expressed in decibels this relationship becomes

$$I_2 = I_1 - 20 \log_{10} \frac{s_2}{s_1} \text{ decibels} \quad (5)$$

where  $\frac{s_2}{s_1}$  is a ratio of the distances. For example, if  $I_1$  is 110 decibels at a distance of 30 feet from a propeller, the sound pressure  $I_2$  at 300 feet is  $110 - 20 \log_{10} \frac{300}{30}$  or 90 decibels.

An additional reduction occurs as a result of atmospheric attenuation, the amount of which is known to vary with the frequency of the sound. For short distances, however, this effect is small.

#### APPARATUS AND METHODS

Static tests for measurement and analysis of noise emission were conducted for five propellers. The propellers tested were the two-blade wooden Sensenich model No. 70D45 propeller, the two-blade NACA 4-(3)(06.3)-06 propeller, and the NACA 4-(3)(08)-03 propeller in two-blade, four-blade, and seven-blade configurations. The NACA designations used give a description of the propeller blade. Numbers in the first group give the propeller diameter in feet. The first number of the second group gives the design lift coefficient, in tenths, at the 0.7 radius. Blade thickness to chord ratio at the 0.7 radius is expressed by the last two digits of the second group. The third group gives blade solidity, which is defined as the ratio of a single blade width at the 0.7 radius to the circumference of a circle with the same radius. The Sensenich propeller is a wooden, fixed-pitch propeller, with a diameter of 5.8 feet. All other types were 4-foot-diameter metal propellers mounted in adjustable hubs which allowed the blade angle to be changed manually. It should be noted that the NACA 4-(3)(06.3)-06 blade and the NACA 4-(3)(08)-03 blade have the same type of airfoil section except for a small difference in thickness and that the solidity of the NACA 4-(3)(06.3)-06 blade is approximately twice that of the NACA 4-(3)(08)-03 blade. Use of these propellers makes it possible to get comparable data for two different solidity values. The inclusion of the Sensenich propeller provides data for a typical light-airplane propeller.

Blade-form curves for the three different blades tested are given in figure 1. Those given for the Sensenich propeller are only approximate since no design data were available and measurements near the tip are difficult to make because of the protective metal leading-edge guard.

A 200-horsepower water-cooled variable-speed electric motor was used to drive the test propellers. Power inputs to the drive motor in all tests were measured directly by means of a wattmeter and these readings were corrected by the use of motor-efficiency data to determine the actual power input to the propeller. The motor was rigidly mounted on an outdoor test stand. (See figs. 2(a) and 2(b).)

The nearest obstructions were located at a distance of about 65 feet from the test stand. Any discrepancies due to reflections are believed to be within the ordinary range of error in measurements for these tests.

A microphone was placed at ground level to insure maximum pick-up of all frequencies and was located at a point 30 feet from the propeller hub and at a  $15^\circ$  angle behind the plane of rotation ( $\beta = 105^\circ$ ). This particular angular position was chosen because it is near the value of  $\beta$  for maximum sound pressures for the range of sound harmonics measured (fig. 1, reference 3).

A survey rake to measure total pressure was clamped to the motor housing at approximately 4 inches behind the propellers. The measured total pressure was integrated over the disk area to obtain an estimate of total thrust. These measurements are believed to be sufficiently accurate ( $\pm 25$  percent) for sound calculations. This error in thrust represents approximately 1 decibel error in sound intensity.

Sound pressures and frequencies were measured with a Western Electric moving-coil pressure-type microphone, associated amplifiers, and a Hewlett Packard Wave Analyzer. An electronic voltmeter measured total microphone voltage. Propeller sounds at each test condition were permanently recorded on disks by means of record-cutting apparatus.

Sound pressures in dynes per square centimeter were measured for the first five harmonics of the fundamental rotational frequency for each test condition. The band width of the wave analyzer used was 25 cycles. Thus a chance for error existed in measurements taken when extraneous frequencies were within this range. Wave-analyzer and microphone-voltmeter readings were corrected for microphone frequency response.

Data were obtained at tip Mach numbers of 0.3, 0.5, 0.7, and 0.9 for all test conditions except as prevented by propeller structural limitations and drive-motor-current and power limitations. Some data were also taken for the Sensenich wooden propeller at propeller rotational speeds of 2100 rpm and 2350 rpm to simulate take-off and cruising-speed conditions. Comparative data for some of the other types of propellers were taken at the same rotational speeds and tip speeds as those of the wooden propeller.

Gusts of wind cause a violent fluctuation in sound pressures for all frequencies of the emitted noise. Measurements on the seven-blade propeller at a  $20^\circ$  blade angle, taken on a day when gusts were approximately 20 miles per hour, showed sound-pressure

variations of approximately 15 decibels at all speeds of the propeller. In order to obtain consistent data, tests were run only on days when wind velocities were low.

## RESULTS AND DISCUSSION

### Sound Pressures

Tests were run on all models (except the two-blade wooden Sensenich propeller) at different pitch settings to vary power absorption at the same tip Mach numbers. Sound pressures were measured at various tip Mach numbers for purposes of comparison. Tables I and II contain all experimental data and calculated values. The tables are useful in comparing theoretical calculations and test data for various operating conditions of the propellers tested. Values shown for wave-analyzer results were obtained by a summation of the sound pressures of the first five harmonics of the fundamental rotational noise frequency as measured by the wave analyzer. Values were also obtained by converting the measured total microphone voltage directly to decibels after the proper microphone calibration was applied. Calculated values obtained from equations (3) and (4) for the first five harmonics are included for comparison with the measured pressures. A sample calculation illustrating the use of equations (3) and (4) is included in the section "SAMPLE CALCULATIONS."

Tables I and II show good agreement between the measured and calculated values at the high Mach numbers for nearly all test conditions. Discrepancies exist at the low Mach numbers for most test conditions and are especially large for the multiblade configurations.

A comparison of the measured data obtained by the two methods for the same test conditions also shows good agreement in most cases at the high Mach numbers but fairly large discrepancies at the low Mach numbers. An analysis of the discrepancies is of interest because of the two different methods of sound measurement. The microphone voltage, when converted to sound pressure, gives the summation of the entire band of frequencies emitted. Wave-analyzer measurements, however, were made only at the rotational noise-frequency peaks. Therefore, if the vortex noise is strong compared with the rotational noise, as is usually the case at low Mach numbers, values determined by microphone voltage will be larger than values determined from wave-analyzer measurements.

Oscillograph records for microphone positions at  $\beta = 0^\circ$  and  $\beta = 90^\circ$  were made for sound emission from a two-blade and a seven-blade propeller. These records appearing in figure 3 show the difference in the quality of sound emitted in these two different directions. Amplifier gains are not the same for all these records and consequently the amplitudes have no meaning. Some estimate of the relative importance of the rotational noise and vortex noise can be made from a study of the records shown. The high-frequency vortex noise is shown to be much stronger in front of each propeller than in the plane of rotation. The reverse is true of the rotational-noise component. The magnitude of the high-frequency component which exists in the plane of rotation is comparatively greater for the seven-blade propeller than for the two-blade propeller. Observations indicate that at  $M_t = 0.50$  for the seven-blade propeller the rotational noise has just begun to dominate the vortex noise. At  $M_t = 0.57$  for the two-blade propeller, rotational noise is clearly dominant.

Several test runs were made with the NACA 4-(3)(08)-03 propeller in two-blade, four-blade, and seven-blade configurations and the results, from tables I and II, are shown in figures 4, 5, and 6. Figures 4 and 5 are plotted with sound-pressure levels against tip speed and figure 6 shows sound-pressure levels plotted against power absorbed for all three configurations. Results indicate that sound-pressure levels in decibels increase approximately as a linear function of tip Mach number; the sound-pressure level increases as more power is absorbed by the propeller. The following table, in which power values that cannot be determined from figure 4 are included for convenience, illustrates measured sound-pressure-level differences for three different blade angles of the two-blade configuration for different tip Mach numbers and powers absorbed:

| $M_t$ | $\theta = 5^\circ$ |               | $\theta = 10^\circ$ |               | $\theta = 16.5^\circ$ |               |
|-------|--------------------|---------------|---------------------|---------------|-----------------------|---------------|
|       | I<br>(db)          | $P_H$<br>(hp) | I<br>(db)           | $P_H$<br>(hp) | I<br>(db)             | $P_H$<br>(hp) |
| 0.3   | 79.8               | 1.0           | 83.4                | 1.4           | 85.8                  | 3.5           |
| .5    | 84.9               | 4.3           | 93.0                | 8.4           | 95.9                  | 20.0          |
| .7    | 100.6              | 15.1          | 105.3               | 27.8          | 110.4                 | 65.8          |
| .9    | 111.1              | 33.4          | 117.0               | 68.2          | 121.6                 | 148.2         |

Figure 5 shows that, at the same tip Mach number and blade angle, sound-pressure levels for a seven-blade configuration are considerably lower than for a similar two-blade configuration.

Curves for the two-blade and four-blade configurations are nearly coincident for most of the Mach number range, even though more power is being absorbed by the four-blade configuration. The cross-over in the curves is probably due to the difference in power absorption. A comparison of the results for the two-, four-, and seven-blade configurations for a constant blade angle of  $16.5^\circ$  is given in the following table:

| $M_t$ | Two-blade |               | Four-blade |               | Seven-blade |               |
|-------|-----------|---------------|------------|---------------|-------------|---------------|
|       | I<br>(db) | $P_H$<br>(hp) | I<br>(db)  | $P_H$<br>(hp) | I<br>(db)   | $P_H$<br>(hp) |
| 0.3   | 85.8      | 3.5           | 81.9       | 6.0           | 78.3        | 10.7          |
| .5    | 95.9      | 20.0          | 96.9       | 34.2          | 89.9        | 53.0          |
| .7    | 110.4     | 65.8          | 111.5      | 110.0         | ----        | ----          |

For equal power consumption at the same blade angle, an increase in the number of blades was found to cause a marked decrease in the sound-pressure levels. (See fig. 6.) A part of this difference is due to a decrease in tip speed.

Figure 7(a) shows comparative data from table I for the NACA 4-(3)(08)-03 two-blade propeller and the NACA 4-(3)(06.3)-06 two-blade propeller. Data for the NACA 4-(3)(06.3)-06 propeller were adjusted to the same tip speed and power absorption as the NACA 4-(3)(06.3)-06 propeller by cross-plotting the data against blade angle. Results indicate that, for operating conditions in which equal amounts of power are absorbed at the same tip speeds, the sound pressures are very nearly equal for the two propellers. This result indicates that blade solidity has very little if any effect on sound emission.

Sound-pressure levels measured by the microphone voltmeter (table I) are plotted against horsepower input to the Sensenich propeller in figure 7(b). Comparative data for two other propellers with entirely different shapes are obtained from cross plots at the same tip speeds and power absorption. Although good agreement was found, no conclusion concerning blade shape can be drawn from this figure because of the differences in diameters and thrust values.

Some test results from the microphone-voltmeter measurements of tables I and II for the two-blade and seven-blade propellers are plotted in figure 8 with the corresponding theoretical curves of total sound-pressure emission as calculated by equations (3) and (4). At the lower Mach numbers the agreement between theory

and experiment is better for the two-blade propeller than for the seven-blade propeller, although, for both, the disagreement between theory and experiment increases as the tip Mach number is reduced. This lack of agreement is caused by the presence of vortex noise which is not accounted for by equation (3).

Wave-analyzer measurements at low Mach numbers confirm the presence of a wide band of frequencies of such strength, in some instances, that no definite rotational-noise peaks exist.

Additional comparisons between theoretical calculations and experimental results are given in figures 9(a) and 9(b). For the two-blade and seven-blade configurations of the NACA 4-(3)(08)-03 propeller at a blade angle of  $10^\circ$  and at tip Mach numbers of 0.3 and 0.9, the plots show the variation of the harmonics of the fundamental rotational frequency ( $qn$ ) with sound-pressure level. There is good agreement over a wide range of frequency at a tip Mach number of 0.9, but large discrepancies exist at a tip Mach number of 0.3 for the same range of frequency.

Experimental results in general show that for all propellers tested the Gutin theory is adequate for prediction of sound pressures in the Mach number range where rotational noise is strong compared with vortex noise.

### Loudness

Sound pressures measured by instrument in many cases do not give a true representation of the loudness of sound as evaluated by the ear. Since the effect of sound on the ear is of prime importance in the study of noise reduction, a brief description of the loudness aspect of sound is presented herein.

Loudness is defined as the magnitude of an auditory sensation. Because of the nonlinear response and the physical characteristics of the vibrating part of the hearing mechanism, sounds at certain amplitudes and frequencies have a masking effect on other sounds. The lower frequencies tend to mask the higher ones.

An empirical formula for calculating the loudness of complex sounds as they would be evaluated by the average ear is given in reference 6 as follows:

$$G(L_n) = \sum_{k=1}^k b_k G(L_k) \quad (6)$$

where

$$b_k = \left( \frac{250 + f_k - f_m}{1000} \right)_{10}^{\left( \frac{L_k - L_m}{U} \right)} z(\psi_k + 30 \log_{10} f_k - 95) \quad (7)$$

Figure 10, which is reproduced from reference 6, shows a chart of loudness-level contours which has been accepted as a standard for the response of the average ear to individual frequencies. Points on the loudness-level contours were determined from the observations of a large group of people. Notes of various frequencies were increased in intensity until they appeared to the observers to be as loud as a 1000-cycle note of known intensity. Figure 10 shows that, for cases where the intensity levels remain of the order of approximately 90 to 120 decibels and at the frequency range of approximately 100 to 1000 cycles per second, the ear evaluates sounds fairly accurately. As the intensity levels decrease, more distortion is evident with a corresponding change in loudness evaluation. For a 1000-cycle note the intensity level is zero decibels at the threshold of hearing and 120 decibels at the threshold of feeling. Figure 10 is replotted for the range from 30 to 4000 cycles per second in figure 11 for convenience in making calculations. Figures 10, 11, and 12, and tables III and IV are reproduced from reference 6 so that two sample problems may be presented. (See section "SAMPLE CALCULATIONS.")

Of great current interest is the comparison of the loudness effects obtained with multiblade propellers with those obtained with conventional two-blade propellers. Figure 13 illustrates the loudness change with distance for three different propellers and for a helicopter rotor. The helicopter data were included to provide a comparison of the loudness effects of such configurations with those of conventional propellers. Sound pressures were first adjusted for distance according to the relationship given in equation (5) and then were converted to a loudness level. No correction for atmospheric attenuation was made.

Figure 13 shows that the advantage to be gained by adding more blades for the same tip speed and power absorption is small at distances greater than 400 feet. For the case of 2 two-blade propellers operating at the same tip speed and power absorption, the one having the larger diameter tends to be less loud because of the lower frequency. The helicopter rotor has a very low loudness level at a distance of 30 feet and at a slightly greater distance becomes inaudible. In general the lower frequencies of sound tend to have greater attenuation in loudness with distance than do the higher ones.



## SAMPLE CALCULATIONS

The following calculation, made by use of equations (3) and (4), is presented to illustrate the method used in obtaining the calculated values in tables I and II. Conditions for a typical problem are as follows:

Propeller radius, feet . . . . . 2  
 Tip Mach number,  $M_t$  . . . . . 0.9  
 Thrust,  $T$ , pounds . . . . . 307.6  
 Power to propeller,  $P_H$ , horsepower . . . . . 106.4  
 Number of blades,  $n$  . . . . . 4  
 Harmonic of rotational frequency,  $q$  . . . . . 1, 2, 3, . . . etc.  
 Distance from propeller,  $L$ , feet . . . . . 30

Evaluating equation (3) gives

$$p_1 = 145 \, qn \, J_{qn}(x)$$

The function  $J_{qn}(x)$  is evaluated from faired curves plotted from Bessel function tables given in reference 7. The steps followed in obtaining  $p_T$  are illustrated in the following table:

| $q$ | $qn$ | $x$   | $J_{qn}(x)$ | $qn \, J_{qn}(x)$ | $p_1$ | $p_T = \sqrt{\sum_{q=1}^5 p_1^2}$ |
|-----|------|-------|-------------|-------------------|-------|-----------------------------------|
| 1   | 4    | 2.78  | 0.121       | 0.484             | 70.1  | 90.1                              |
| 2   | 8    | 5.56  | .039        | .318              | 46.1  |                                   |
| 3   | 12   | 8.34  | .016        | .194              | 28.2  |                                   |
| 4   | 16   | 11.12 | .006        | .105              | 15.3  |                                   |
| 5   | 20   | 13.90 | .0026       | .053              | 7.8   |                                   |

From equation (4), the value of  $I$  is obtained as

$$\begin{aligned} I &= 74 + 20 \log_{10} p_T \\ &= 113.1 \text{ decibels} \end{aligned}$$

Applying a ground-reflection correction of 6 decibels gives

$$\begin{aligned} I &= 113.1 + 6.0 \\ &= 119.1 \text{ decibels} \end{aligned}$$

Sample calculations are made to illustrate the use of equation (6). The following tabulation gives the total loudness of a two-blade propeller at a distance of 30 feet:

| Harmonic,<br>$k$ | $f_k$ | $\psi_k$ | $L_k$ | $G_k$ | $b_k$ | $b_k G_k$   | $L_n$<br>(db) | Contribution<br>(percent) |
|------------------|-------|----------|-------|-------|-------|-------------|---------------|---------------------------|
| 1                | 127   | 64.6     | 52    | 2510  | 1.0   | 2510        |               | 32.2                      |
| 2                | 254   | 62.7     | 58    | 3220  | .762  | 2910        |               | 38.1                      |
| 3                | 381   | 59.1     | 57    | 3560  | .346  | 1232        |               | 16.1                      |
| 4                | 508   | 55.6     | 55    | 3080  | .323  | 995         |               | 13.0                      |
|                  |       |          |       |       |       | 7647 = 69.4 |               |                           |

The first column  $k$  contains the order of the component. The number of blade tips passing a given point per second is the first harmonic, and the other harmonics are integral multiples of it. If the values  $f_k$  and  $\psi_k$  are measured directly, the corresponding values of  $L_k$  can be found from figure 11; then the loudness values  $G_k$  are found in table III. The masking factor  $b_k$  is determined by the use of equation (7), with the aid of figure 12 and table IV. This factor  $b_k$  can never be greater than unity and unity is used whenever calculations give a higher value. The component for which the values of  $I_m$ ,  $f_m$ , and  $U$  introduced in equation (7) give the smallest value of  $b_k$  is the masking component. In general, the lower components tend to mask those directly higher. The product of  $b_k$  and  $G_k$  gives the relative loudness of the individual components. The summation of all the individual values of  $b_k G_k$  is the loudness of the complex tone. The corresponding loudness level  $L_n$  is found from table III.

In the following table, calculations are presented for a three-blade helicopter rotor at a distance of 30 feet to illustrate two extremes in the use of the loudness-level-contour chart (fig. 11):

| Harmonic,<br>$k$ | $f_k$ | $\psi_k$ | $L_k$ | $G_k$ | $b_k$ | $b_k G_k$ | $L_n$<br>(db) | Contribution<br>(percent) |
|------------------|-------|----------|-------|-------|-------|-----------|---------------|---------------------------|
| 1                | 13.7  | 90.6     | 0     | 0     | 0     | 0         |               | 0                         |
| 2                | 27.4  | 74.5     | 20    | 97.5  | 1.0   | 97.5      |               | 100                       |
| 3                | 41.1  | 56.3     | 0     | 0     | 0     | 0         |               | 0                         |
|                  |       |          |       |       |       | 97.5 = 20 |               |                           |

The frequency of the fundamental is noted to be 13.7 cycles per second, which is inaudible. Hence, even though a large amount of sound energy is emitted, the corresponding loudness value is zero. The intensity level of the third harmonic is so low that at its particular frequency of sound it is below the threshold of hearing and also has a corresponding loudness value of zero. In this particular illustration all of the loudness is contributed by the second harmonic of the rotational frequency.

### CONCLUSIONS

Sound-pressure measurements at static conditions of two-blade, four-blade, and seven-blade propellers in the tip Mach number range from 0.3 to 0.9 indicate the following conclusions:

1. At a constant pitch setting, the sound pressure in decibels for a given propeller varies in an approximately linear manner with the tip speed of the propeller for the range of test Mach number.
2. At the same tip speed, diameter, and power absorbed, the sound-pressure outputs of two-blade propellers are approximately equal and are not influenced by solidity.
3. For the propellers tested, the Gutin theory is adequate for the prediction of total sound pressures for the Mach number range where rotational noise is strong compared with vortex noise, as is the case for two-blade propellers.
4. An appreciable sound-pressure reduction can be attained for given operating conditions by increasing the number of propeller blades, but the reduction will be less than that predicted by Gutin's theory when vortex noise is a large part of the total noise. Vortex noise is a large part of the total noise at low tip Mach numbers, especially for multiblade propellers and, therefore, Gutin's formula will be inaccurate for these conditions.
5. In general, the lower frequencies of sound tend to have greater attenuation in loudness with distance than do the higher ones. As a result, for the same tip speed and power absorbed, the seven-blade propeller tested is only slightly less loud than a two-blade propeller at a distance greater than 400 feet, even though the difference in sound pressures is large. For the same tip speed

and power absorbed a small reduction in loudness may be realized by increasing the diameter.

Langley Memorial Aeronautical Laboratory  
National Advisory Committee for Aeronautics  
Langley Field, Va., May 7, 1947

#### REFERENCES

1. Theodorsen, Theodore, and Regier, Arthur A.: The Problem of Noise Reduction with Reference to Light Airplanes. NACA TN No. 1145, 1946.
2. Gutin, L.: Über das Schallfeld einer rotierenden Luftschraube. Phys. Zeitschr. der Sowjetunion, Bd. 9, Heft 1, 1936, pp. 57-71.
3. Deming, Arthur F.: Propeller Rotation Noise Due to Torque and Thrust. NACA TN No. 747, 1940.
4. Stowell, E. Z., and Deming, A. F.: Vortex Noise from Rotating Cylindrical Rods. NACA TN No. 519, 1935.
5. Anon.: American Tentative Standard Acoustical Terminology. ASA Z24.1, American Standards Assoc., 1936.
6. Fletcher, Harvey, and Munson, W. A.: Loudness, Its Definition, Measurement and Calculation. Jour. Acous. Soc. Am., vol. V, no. 2, Oct. 1933, pp. 82-108.
7. Jahnke, Eugene, and Emde, Fritz: Tables of Functions with Formulae and Curves. Rev. ed. Dover Publications (New York), 1943.

TABLE I  
SUMMARY OF DATA FOR TWO-BLADE PROPELLERS

| Blade angle at $0.75R_t$ (deg) | Propeller rotational speed (rpm) | Tip Mach number, $M_t$ | Estimated thrust (lb) | Power input to propeller (hp) | Total sound-pressure level measured by wave analyzer (db) | Total sound-pressure level measured by microphone voltmeter (db) | Total sound-pressure level calculated by formulas (3) and (4) |
|--------------------------------|----------------------------------|------------------------|-----------------------|-------------------------------|---|--|---|
| NACA 4-(3)(08)-03              |                                  |                        |                       |                               |   |  |   |
| 16.5                           | 1600                             | 0.3                    | 27.9                  | 3.5                           | 79.6  | 85.8   | 83.8  |
|                                | 2680                             | .5                     | 65.1                  | 20.0                          | 95.9  | 95.9   | 98.0  |
|                                | 3770                             | .7                     | 177.4                 | 65.8                          | 111.4   | 110.4  | 111.1   |
|                                | 4850                             | .9                     | 316.4                 | 148.2                         | 123.4   | 121.6  | 123.0   |
| 10.0                           | 1600                             | .3                     | 9.1                   | 1.4                           | 78.7  | 83.4   | 71.4  |
|                                | 2680                             | .5                     | 32.9                  | 8.4                           | 92.6  | 93.0   | 89.3  |
|                                | 3770                             | .7                     | 61.6                  | 27.8                          | 107.4   | 105.3  | 103.1   |
|                                | 4850                             | .9                     | 184.0                 | 68.2                          | 119.3   | 117.0  | 117.8   |
| 5.0                            | 1600                             | .3                     | 9.3                   | 1.0                           | 73.8  | 79.8   | 69.3  |
|                                | 2680                             | .5                     | 24.1                  | 4.3                           | 89.1  | 89.9   | 84.3  |
|                                | 3770                             | .7                     | 53.0                  | 15.1                          | 101.5   | 100.6  | 98.9  |
|                                | 4850                             | .9                     | 95.0                  | 33.4                          | 114.3   | 111.1  | 111.8   |
| 12.0                           | 1600                             | .3                     | 18.6                  | 3.0                           | 77.6  | 80.8   | 74.1  |
|                                | 2680                             | .5                     | 53.6                  | 12.6                          | 95.1  |  | 92.6  |
|                                | 3770                             | .7                     | 104.6                 | 38.0                          | 108.5   | 106.3  | 106.5   |
|                                | 4850                             | .9                     | 184.3                 | 90.6                          | 120.9   | 119.6  | 119.5   |
| NACA 4-(3)(06.3)-06            |                                  |                        |                       |                               |   |  |   |
| 16.5                           | 1600                             | 0.3                    | 41.0                  | 4.6                           | 82.8  | 83.4   | 78.3  |
|                                | 2680                             | .5                     | 128.0                 | 33.7                          | 98.9  | 99.0   | 100.1   |
|                                | 3770                             | .7                     | 230.0                 | 92.8                          | 113.7   | 112.3  | 110.3   |
|                                | 4300                             | .8                     | 290.0                 | 145.8                         | 119.5   | 118.1  | 120.9   |
| 10.0                           | 1600                             | .3                     | 25.8                  | 1.9                           | 80.9  | 79.8   | 75.2  |
|                                | 2680                             | .5                     | 65.7                  | 12.3                          | 93.1  | 93.0   | 93.2  |
|                                | 3770                             | .7                     | 156.0                 | 54.6                          | 108.2   | 106.6  | 107.4   |
|                                | 4300                             | .8                     | 195.0                 | 59.8                          | 114.4   | 111.0  | 113.9   |
| 5.0                            | 1600                             | .3                     | 7.4                   | 1.0                           | 76.4  | 79.8   | 68.4  |
|                                | 2680                             | .5                     | 38.0                  | 6.0                           | 90.3  | 92.1   | 87.3  |
|                                | 3770                             | .7                     | 86.0                  | 19.3                          | 106.5   | 104.4  | 101.8   |
|                                | 4300                             | .8                     | 118.0                 | 31.2                          | 111.0   | 108.9  | 108.8   |
| Sensenich                      |                                  |                        |                       |                               |   |  |   |
| 12.8                           | 1100                             | 0.3                    | 52.9                  | 3.5                           | 80.8  | 83.5   | 77.5  |
|                                | 1840                             | .5                     | 143.4                 | 23.5                          | 96.3  | 96.6   | 95.8  |
|                                | 2100                             | .57                    | 186.6                 | 40.2                          | 101.4   | 98.3   | 101.6   |
|                                | 2300                             | .625                   | 225.8                 | 57.0                          | 105.5   | 103.1  | 105.5   |

TABLE II  
SUMMARY OF DATA FOR FOUR- AND SEVEN-BLADE  
NACA 4-(3)(08)-03 PROPELLERS

| Blade angle at $0.75R_t$ (deg) | Propeller rotational speed (rpm) | Tip Mach number, $M_t$ | Estimated thrust (lb) | Power input to propeller (hp) | Total sound-pressure level measured by wave analyzer (db) | Total sound-pressure level measured by microphone voltmeter (db) | Total sound-pressure level calculated by formulas (3) and (4) |
|--------------------------------|----------------------------------|------------------------|-----------------------|-------------------------------|---|--|---|
| Seven-blade propeller          |                                  |                        |                       |                               |   |  |   |
| 25.0                           | 1600                             | 0.3                    | 56.9                  | 22.7                          | 82.8  | 86.8   | 44.5  |
|                                | 2140                             | .4                     | 146.3                 | 61.2                          | 87.3  | 92.8   | 69.7  |
|                                | 2300                             | .43                    | 154.2                 | 79.0                          | 90.6  | 95.9   | 75.6  |
| 21.5                           | 1600                             | .3                     | 85.0                  | 19.3                          | 76.2  | 91.5   | 43.5  |
|                                | 2140                             | .4                     | 155.4                 | 48.0                          | 80.4  | 92.8   | 67.8  |
|                                | 2300                             | .43                    | 180.0                 | 61.2                          | 83.6  | 94.0   | 73.8  |
|                                | 2680                             | .5                     | 243.0                 | 99.0                          | 92.3  | 99.5   | 85.5  |
|                                | 2780                             | .52                    | 250.0                 | 110.0                         | 92.5  | 102.0  | 86.3  |
| 20.0                           | 1600                             | .3                     | 72.4                  | 15.6                          | 77.1  | 86.8   | 51.1  |
|                                | 2140                             | .4                     | 164.1                 | 37.0                          | 82.4  | 92.8   | 65.8  |
|                                | 2680                             | .5                     | 227.0                 | 77.4                          | 93.8  | 102.0  | 83.5  |
|                                | 3080                             | .575                   | 296.9                 | 121.0                         | 97.9  | 105.5  | 93.6  |
| 16.5                           | 1600                             | .3                     | 79.4                  | 10.7                          | 68.8  | 78.3   | 38.4  |
|                                | 2680                             | .5                     | 238.3                 | 53.0                          | 85.0  | 89.9   | 80.9  |
|                                | 3450                             | .64                    | 413.5                 | 124.0                         | 99.2  | 100.0  | 98.6  |
| 12.0                           | 1600                             | .3                     | 51.7                  | 6.3                           | 69.7  | 80.0   | 35.4  |
|                                | 2140                             | .4                     | 92.2                  | 16.4                          | 79.6  | 85.5   | 59.2  |
|                                | 2680                             | .5                     | 146.0                 | 33.0                          | 84.2  | 89.9   | 75.2  |
|                                | 3770                             | .7                     | 314.0                 | 97.6                          | 101.7   | 101.0  | 101.2   |
| 10.0                           | 1600                             | .3                     | 51.5                  | 4.2                           | 63.1  | 75.9   | 31.2  |
|                                | 2680                             | .5                     | 146.8                 | 25.0                          | 80.1  | 88.0   | 75.0  |
|                                | 3770                             | .7                     | 289.6                 | 76.0                          | 101.1   | 101.0  | 100.3   |
|                                | 4850                             | .9                     | 509.7                 | 169.0                         | 120.2   | 119.5  | 119.1   |
| Four-blade propeller           |                                  |                        |                       |                               |   |  |   |
| 16.5                           | 1600                             | 0.3                    | 46.5                  | 6.0                           | 75.8  | 81.9   | 65.76   |
|                                | 2680                             | .5                     | 140.5                 | 34.2                          | 94.3  | 96.9   | 90.9  |
|                                | 3770                             | .7                     | 283.0                 | 110.0                         | 110.6   | 111.5  | 110.5   |
|                                | 4300                             | .8                     | 420.6                 | 167.8                         | 116.8   | 116.4  |   |
| 10.0                           | 1600                             | .3                     | 20.4                  | 2.3                           | 74.2  | 75.9   | 56.0  |
|                                | 2680                             | .5                     | 63.6                  | 14.4                          | 88.2  | 89.0   | 83.7  |
|                                | 3770                             | .7                     | 165.6                 | 41.4                          | 105.0   | 105.1  | 103.1   |
|                                | 4850                             | .9                     | 307.6                 | 106.4                         | 120.4   | 120.2  | 119.1   |
| 5.0                            | 1600                             | .3                     | 12.3                  | 1.0                           | 72.8  | 78.8   | 49.5  |
|                                | 2680                             | .5                     | 40.7                  | 7.4                           | 84.0  | 89.0   | 78.5  |
|                                | 3770                             | .7                     | 81.4                  | 23.3                          | 99.1  | 99.5   | 97.7  |

TABLE III  
VALUES OF  $G(L_K)$

[Table taken from reference 6]

| $L_n$ | 0      | 1      | 2      | 3      | 4      | 5      | 6      | 7       | 8       | 9       |
|-------|--------|--------|--------|--------|--------|--------|--------|---------|---------|---------|
| -10   | 0.015  | 0.025  | 0.04   | 0.06   | 0.09   | 0.14   | 0.22   | 0.32    | 0.45    | 0.70    |
| 0     | 1.00   | 1.40   | 1.90   | 2.51   | 3.40   | 4.43   | 5.70   | 7.08    | 9.00    | 11.2    |
| 10    | 13.9   | 17.2   | 21.4   | 26.6   | 32.6   | 39.3   | 47.5   | 57.5    | 69.5    | 82.5    |
| 20    | 97.5   | 113    | 131    | 151    | 173    | 197    | 222    | 252     | 287     | 324     |
| 30    | 360    | 405    | 455    | 505    | 555    | 615    | 675    | 740     | 810     | 890     |
| 40    | 975    | 1060   | 1155   | 1250   | 1360   | 1500   | 1640   | 1780    | 1920    | 2070    |
| 50    | 2200   | 2350   | 2510   | 2680   | 2880   | 3080   | 3310   | 3560    | 3820    | 4070    |
| 60    | 4350   | 4640   | 4950   | 5250   | 5560   | 5870   | 6240   | 6620    | 7020    | 7440    |
| 70    | 7950   | 8510   | 9130   | 9850   | 10600  | 11400  | 12400  | 13500   | 14600   | 15800   |
| 80    | 17100  | 18400  | 19800  | 21400  | 23100  | 25000  | 27200  | 29600   | 32200   | 35000   |
| 90    | 38000  | 41500  | 45000  | 49000  | 53000  | 57000  | 62000  | 67500   | 74000   | 81000   |
| 100   | 88000  | 97000  | 106000 | 116000 | 126000 | 138000 | 150000 | 164000  | 180000  | 197000  |
| 110   | 215000 | 235000 | 260000 | 288000 | 316000 | 346000 | 380000 | 418000  | 460000  | 506000  |
| 120   | 556000 | 609000 | 668000 | 732000 | 800000 | 875000 | 956000 | 1047000 | 1150000 | 1266000 |

NATIONAL ADVISORY  
COMMITTEE FOR AERONAUTICS

TABLE IV  
VALUES OF  $z(x)$

[Table taken from reference 6]

| $x$<br>(a) | 0    | 1    | 2    | 3    | 4    | 5    | 6    | 7    | 8    | 9    |
|------------|------|------|------|------|------|------|------|------|------|------|
| 0          | 5.00 | 4.88 | 4.76 | 4.64 | 4.53 | 4.41 | 4.29 | 4.17 | 4.05 | 3.94 |
| 10         | 3.82 | 3.70 | 3.58 | 3.46 | 3.35 | 3.33 | 3.11 | 2.99 | 2.87 | 2.76 |
| 20         | 2.64 | 2.52 | 2.40 | 2.28 | 2.16 | 2.05 | 1.95 | 1.85 | 1.76 | 1.68 |
| 30         | 1.60 | 1.53 | 1.47 | 1.40 | 1.35 | 1.30 | 1.25 | 1.20 | 1.16 | 1.13 |
| 40         | 1.09 | 1.06 | 1.03 | 1.01 | .99  | .97  | .95  | .94  | .92  | .91  |
| 50         | .90  | .90  | .89  | .89  | .88  | .88  | .88  | .88  | .88  | .88  |
| 60         | .88  | .88  | .88  | .88  | .88  | .88  | .88  | .89  | .89  | .90  |
| 70         | .90  | .91  | .92  | .93  | .94  | .96  | .97  | .99  | 1.00 | 1.02 |
| 80         | 1.04 | 1.06 | 1.08 | 1.10 | 1.13 | 1.15 | 1.17 | 1.19 | 1.22 | 1.24 |
| 90         | 1.27 | 1.29 | 1.31 | 1.34 | 1.36 | 1.39 | 1.41 | 1.44 | 1.46 | 1.48 |
| 100        | 1.51 | 1.53 | 1.55 | 1.58 | 1.60 | 1.62 | 1.64 | 1.67 | 1.69 | 1.71 |

<sup>a</sup> $x = \psi_k + 30 \log f_k - 95.$

NATIONAL ADVISORY  
COMMITTEE FOR AERONAUTICS



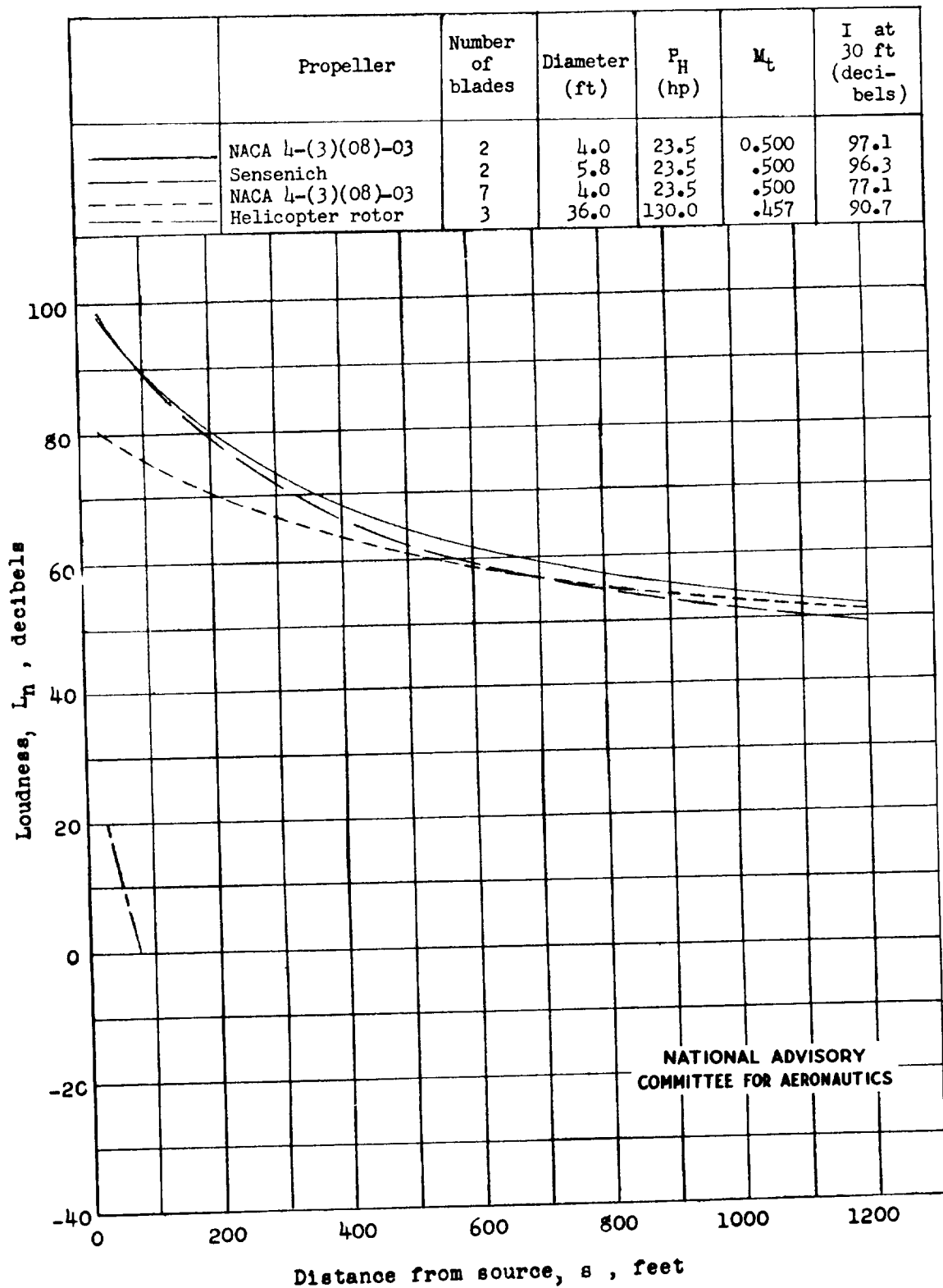


Figure 13.- Comparison of distance effects on propeller loudness.



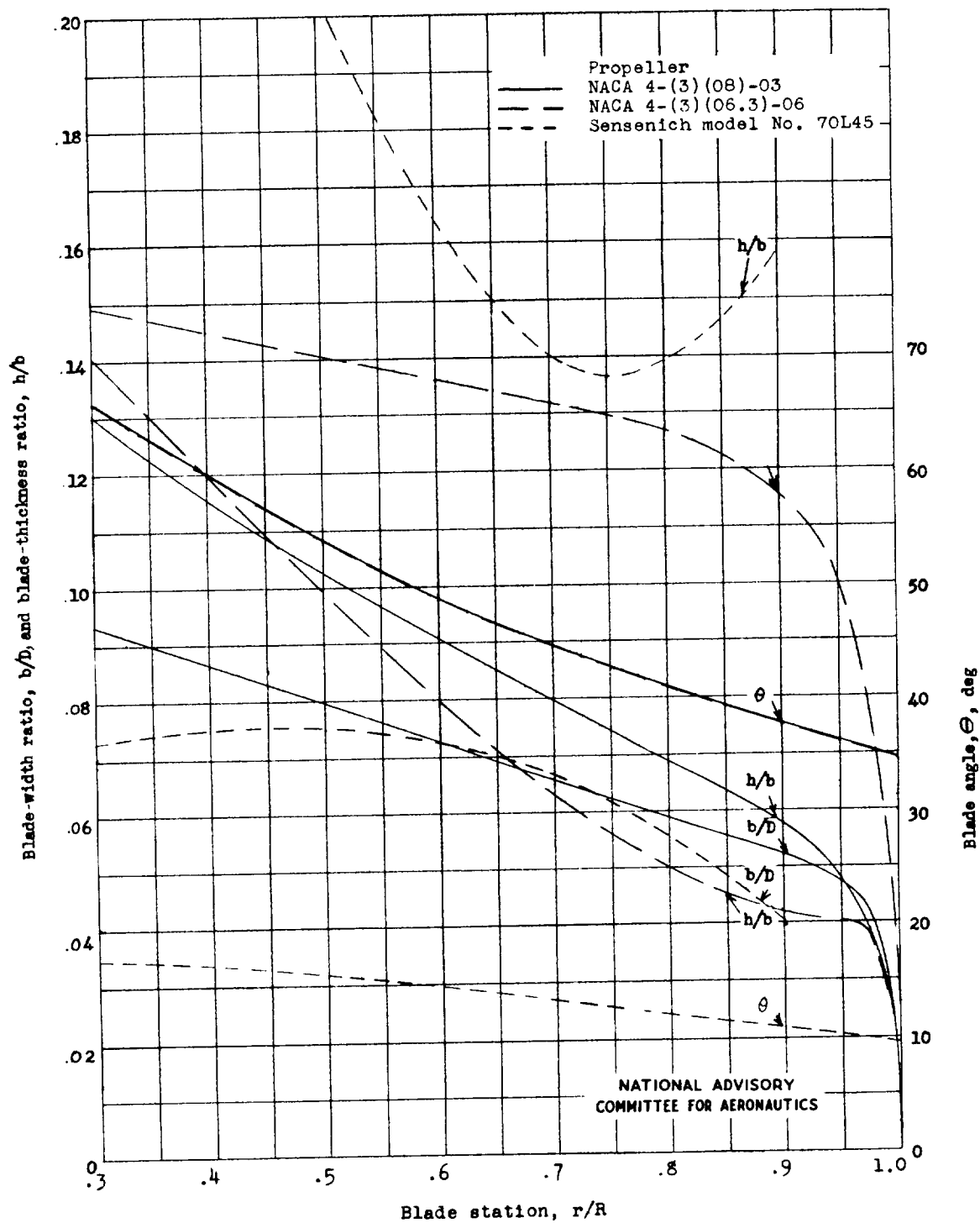


Figure 1.- Blade-form curves for propellers tested.

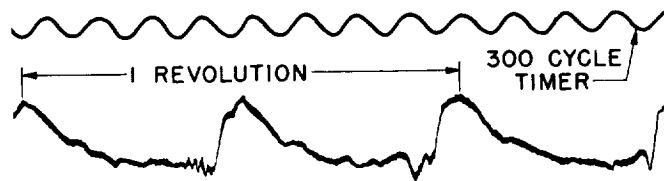




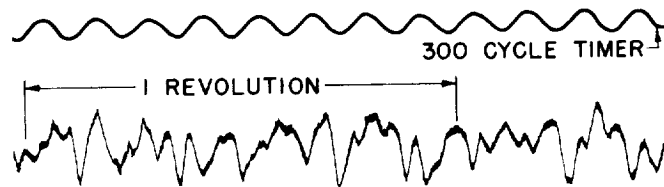
(a) Seven-blade NACA 4-(3)(08)-03 propeller mounted on test stand.

Figure 2.- Setup at Langley sound laboratory for sound-emission tests.

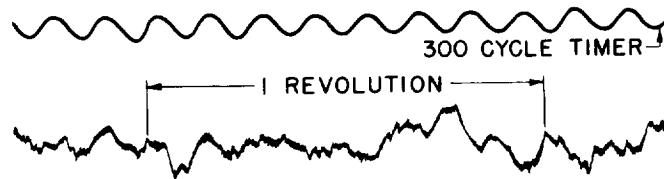




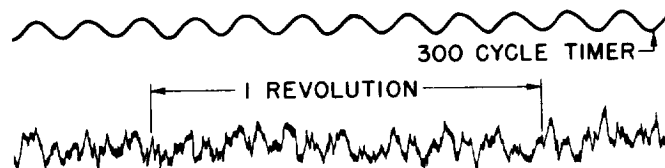
(a) TWO-BLADE SENSENICH PROPELLER.  $M_t = 0.57$ ,  $\beta = 90^\circ$ .



(b) TWO-BLADE SENSENICH PROPELLER.  $M_t = 0.57$ ,  $\beta = 0^\circ$ .



(c) SEVEN-BLADE NACA 4-(3)(08)-03 PROPELLER.  $M_t = 0.5$ ,  $\theta = 16.5^\circ$ ,  $\beta = 90^\circ$ .



(d) SEVEN-BLADE NACA 4-(3)(08)-03 PROPELLER.  $M_t = 0.5$ ,  $\theta = 16.5^\circ$ ,  $\beta = 0^\circ$ .

NATIONAL ADVISORY  
COMMITTEE FOR AERONAUTICS

Figure 3.- Oscillograph records of sound emission of two- and seven-blade propellers.

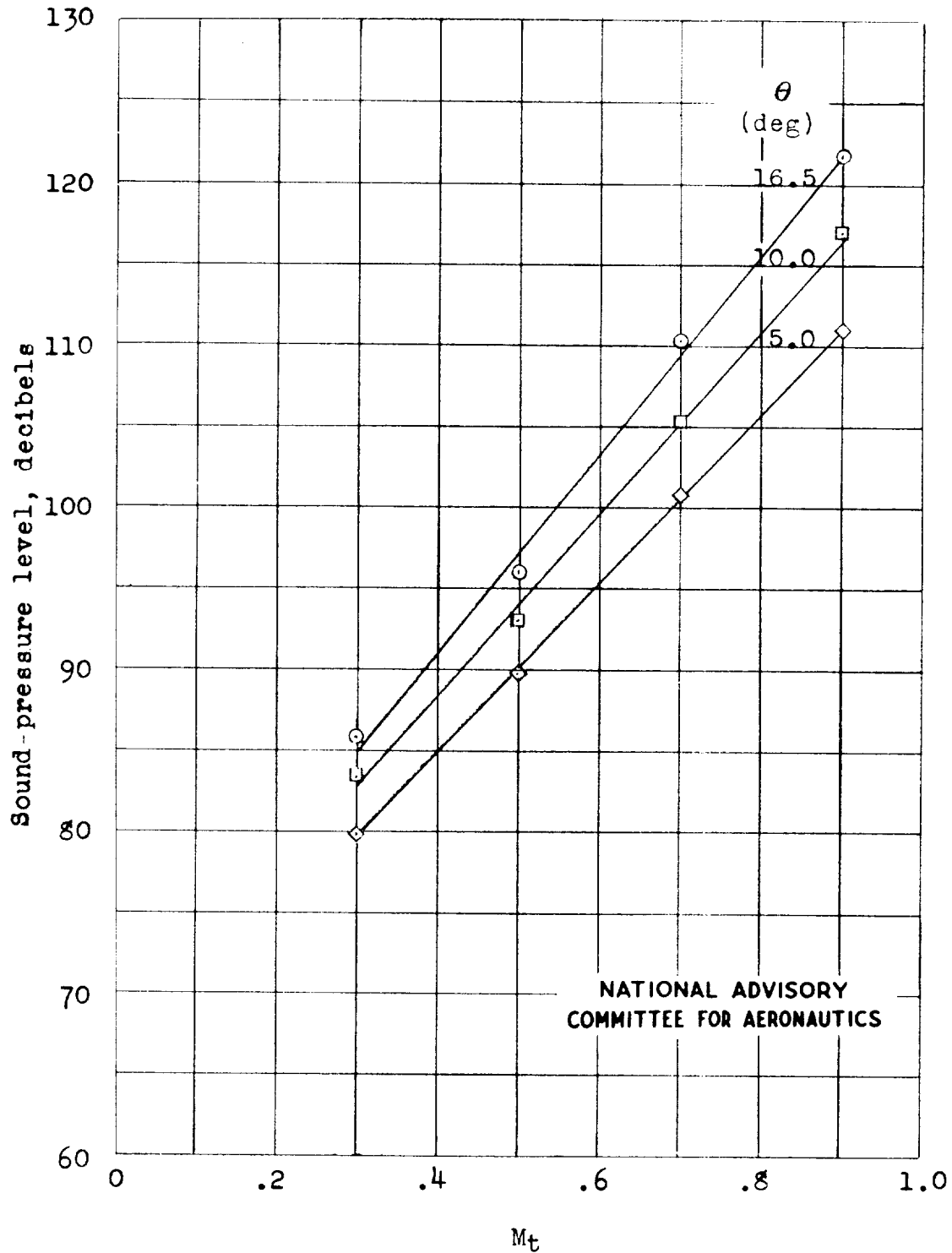


Figure 4.- Variation with tip Mach number and blade angle of sound-pressure level for two-blade NACA 4-(3)(08)-03 propeller.



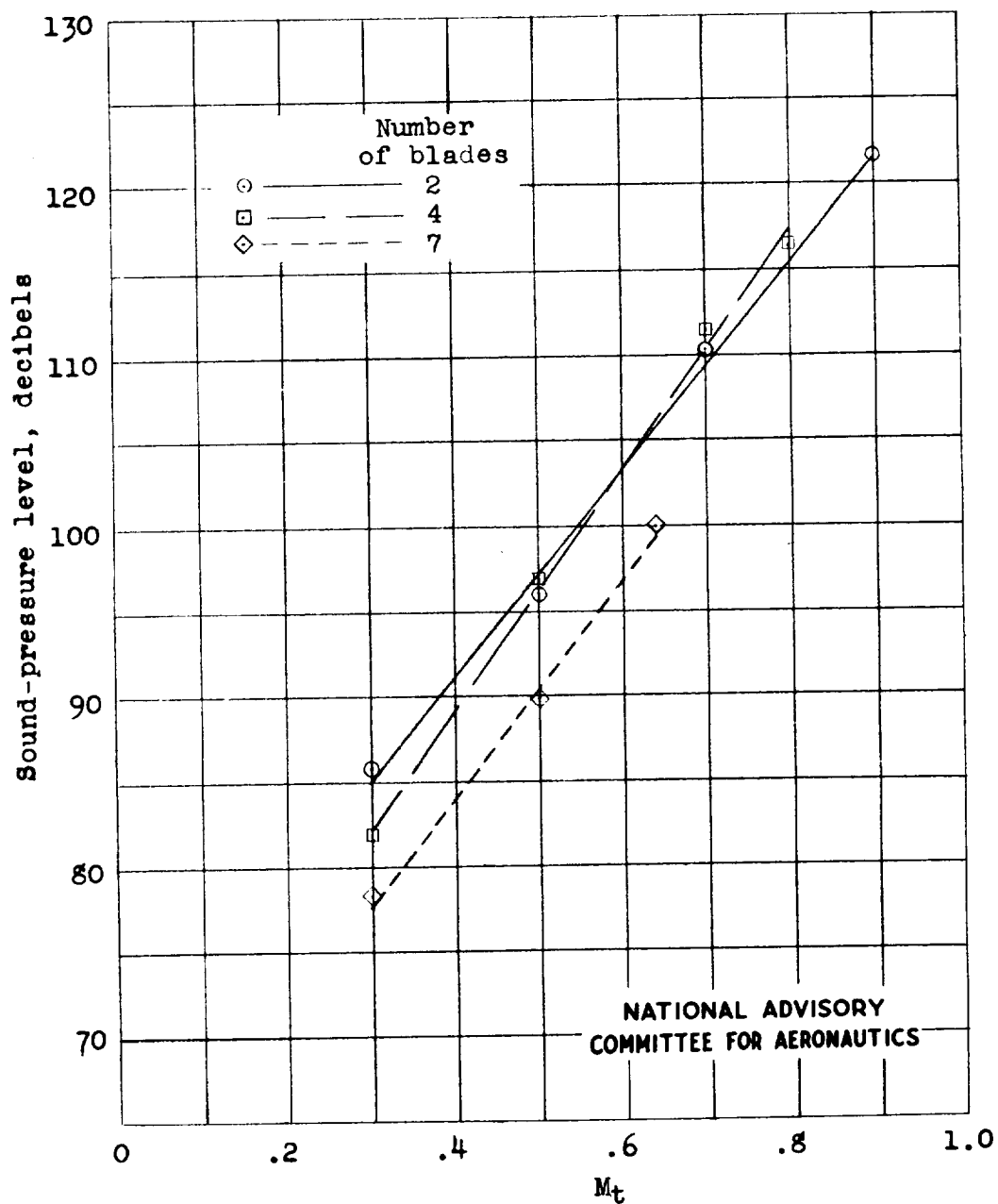


Figure 5.- Effect of number of blades on variation of sound-pressure levels with Mach number for NACA 4-(3)(08)-03 propeller with blade angle  $\theta = 16.5^\circ$ .

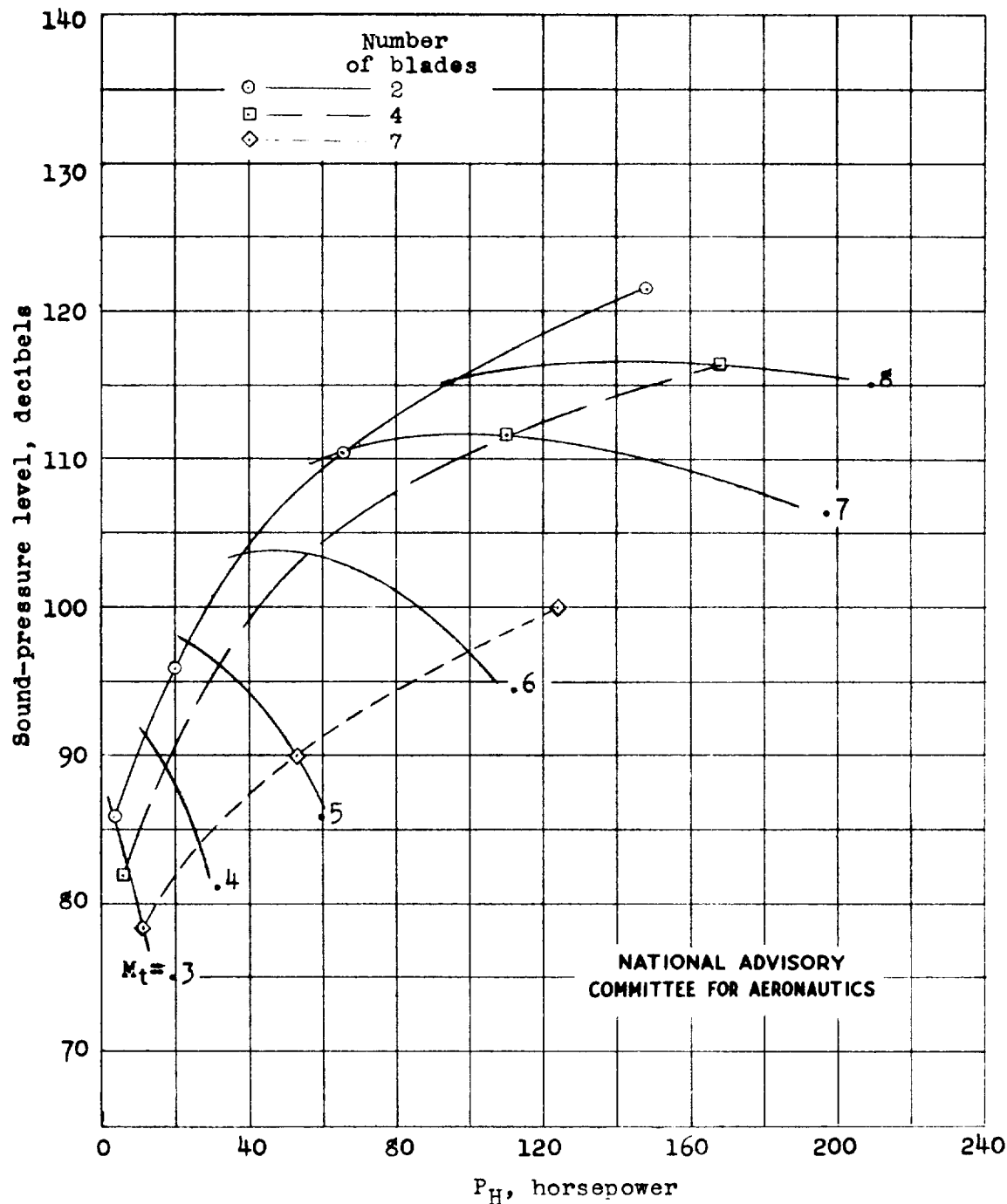
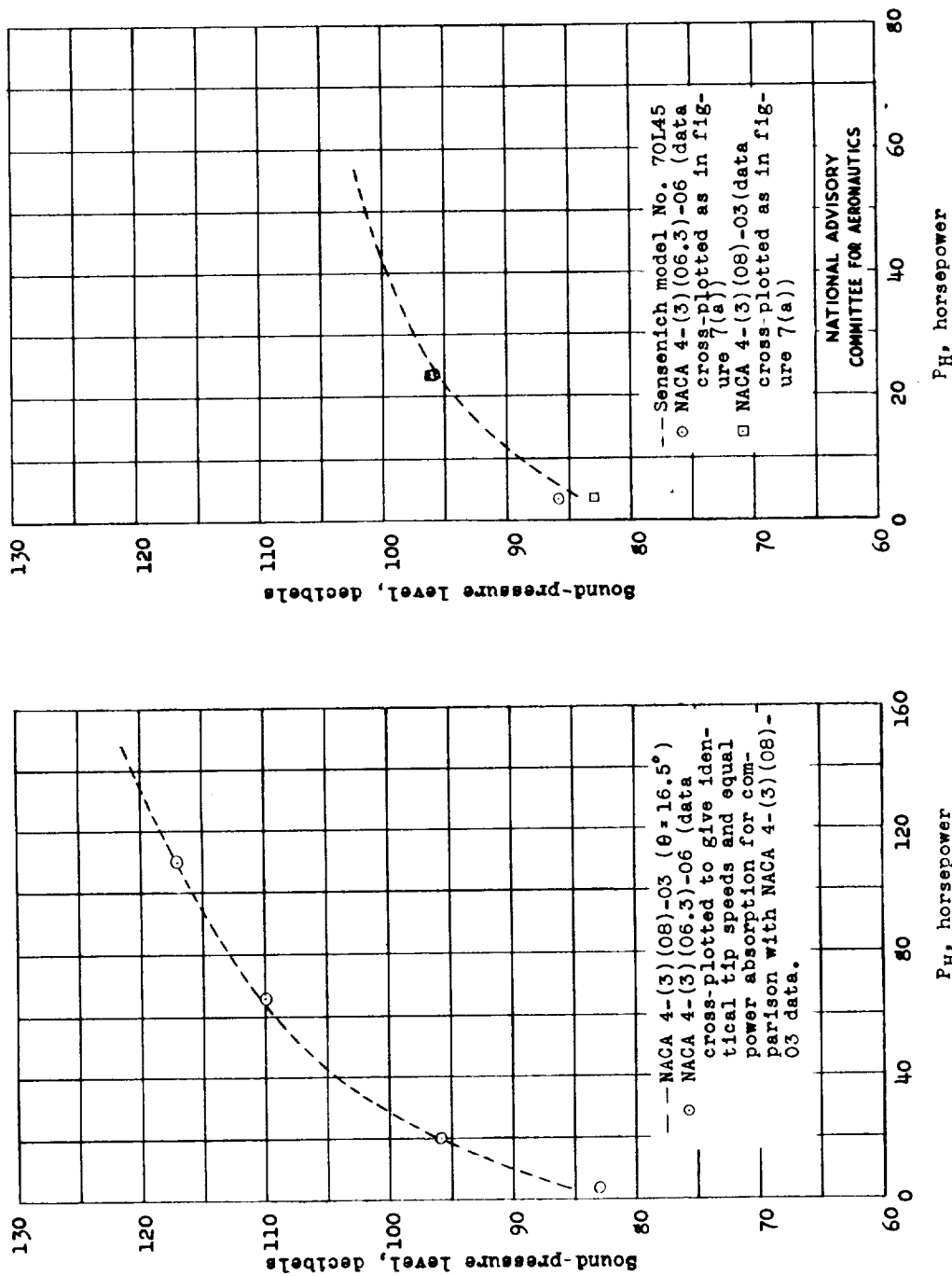


Figure 6.- Effect of number of blades and Mach number on variation of sound-pressure levels with power input for NACA 4-(3)(08)-03 propeller with blade angle  $\theta = 16.5^\circ$ .



(b) Effect of blade shape.

(a) Effect of solidity.

Figure 7.- Comparative data for three different two-blade propellers showing effect of blade shape and solidity on sound emission.

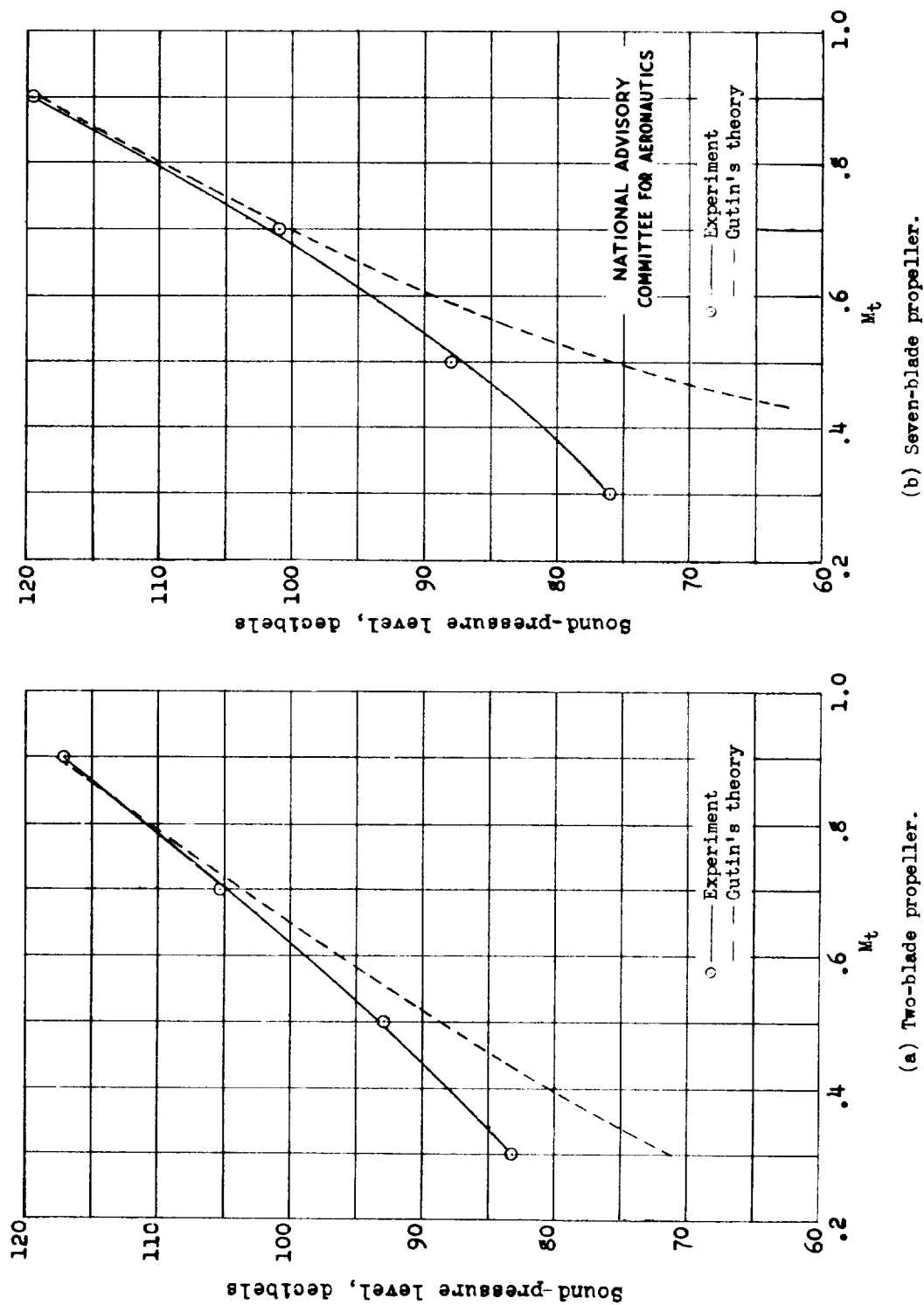


Figure 8.- NACA 4-(3)(08)-03 propeller test data ( $\theta=10^\circ$ ) compared with Gutin's theory.

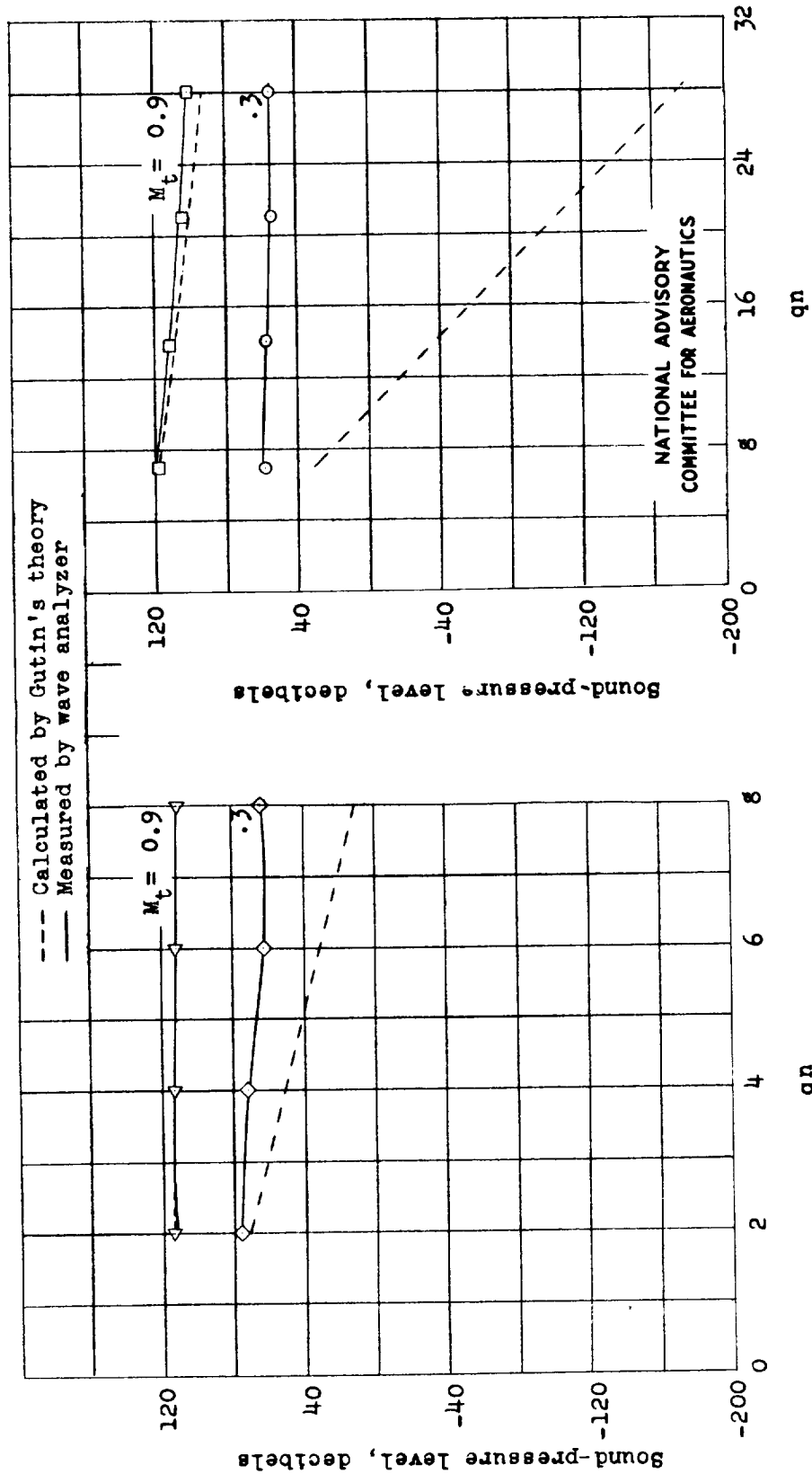


Figure 9.- Sound-pressure emission of NACA 4-(3)(08)-03 propeller.  $\theta = 10^\circ$ .

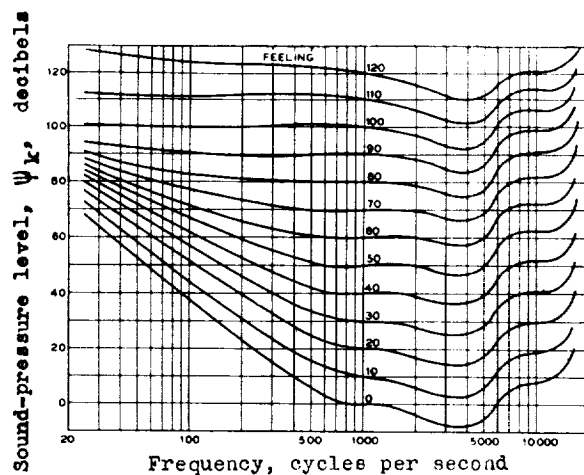


Figure 10.- Loudness-level contours.  
(From reference 6.)

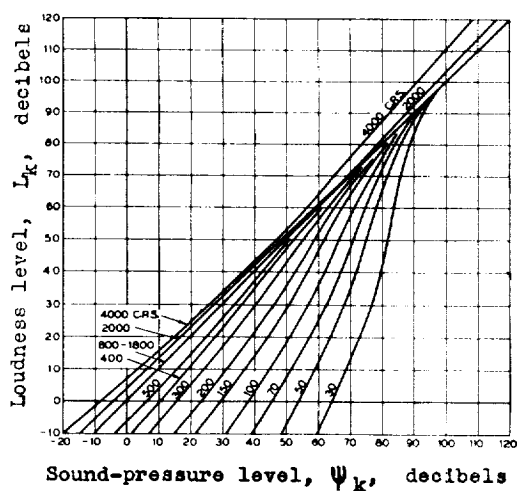


Figure 11.- Loudness levels of pure tones.  
(From reference 6.)

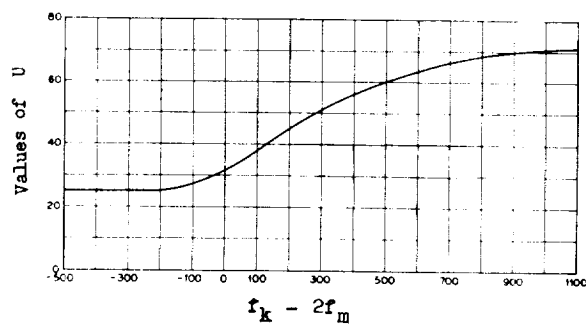


Figure 12.- Values of masking coefficient U.  
(From reference 6.)

NATIONAL ADVISORY  
COMMITTEE FOR AERONAUTICS



(b) Two-blade propeller mounted on test stand.

Figure 2.- Concluded.

